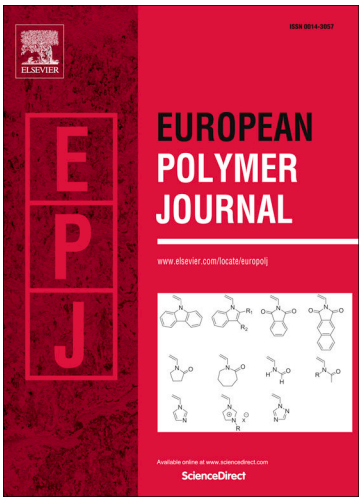

Synthesis and temperature-induced self-assembly of a positively charged symmetrical pentablock terpolymer in aqueous solutions

Erfan Dashtimoghadam, Hamed Salimi-Kenari, Vahid Forooqi Motlaq, Mohammad Mahdi Hasani-Sadrabadi, Hamid Mirzadeh, Kaizheng Zhu, Kenneth D. Knudsen, Bo Nyström

PII: S0014-3057(17)31434-9
DOI: https://doi.org/10.1016/j.eurpolymj.2017.10.008
Reference: EPJ 8107

To appear in: *European Polymer Journal*

Received Date: 13 August 2017
Accepted Date: 8 October 2017

Please cite this article as: Dashtimoghadam, E., Salimi-Kenari, H., Forooqi Motlaq, V., Mahdi Hasani-Sadrabadi, M., Mirzadeh, H., Zhu, K., Knudsen, K.D., Nyström, B., Synthesis and temperature-induced self-assembly of a positively charged symmetrical pentablock terpolymer in aqueous solutions, *European Polymer Journal* (2017), doi: https://doi.org/10.1016/j.eurpolymj.2017.10.008

Synthesis and temperature-induced self-assembly of a positively charged symmetrical pentablock terpolymer in aqueous solutions

Erfan Dashtimoghadam [a,b], Hamed Salimi-Kenari [c], Vahid Forooqi Motlaq [a], Mohammad Mahdi Hasani-Sadrabadi [d], Hamid Mirzadeh [e], Kaizheng Zhu [a], Kenneth D. Knudsen [f], Bo Nyström [a,*]

[a] *Department of Chemistry, University of Oslo, Oslo, Norway.*

[b] *Department of Chemistry, University of North Carolina, Chapel Hill, NC 27599, USA.*

[c] *Faculty of Engineering & Technology, University of Mazandaran, Babolsar, Iran.*

[d] *Parker H. Petit Institute for Bioengineering and Bioscience, and G.W. Woodruff School of Mechanical Engineering, Georgia Institute of Technology, Atlanta, GA, USA.*

[e] *Department of Polymer Engineering and Color Technology, Amirkabir University of Technology, Tehran, Iran.*

[f] *Department of Physics, Institute for Energy Technology, P.O. Box 40, N-2027 Kjeller, Norway*

ABSTRACT

A novel linear cationic ABCBA pentablock terpolymer composed of a positively charged poly (3-acrylamidopropyl) trimethyl ammonium chloride)) (PAMPTMA (+)) block at both ends and two thermoresponsive poly (*N*-isopropylacrylamide) (PNIPAAM) blocks separated by a hydrophilic poly(ethylene glycol) (PEG) block was synthesized *via* a "one-pot" atom transfer radical polymerization procedure (ATRP). The chemical composition of the pentablock terpolymer was confirmed by nuclear magnetic resonance (NMR) and asymmetric flow field-flow fractionation (AFFFF). Depending on the polymer concentration in aqueous

solution, this terpolymer forms unimers and self-assembled structures at elevated temperatures. The effect of concentration and temperature-induced self-assembling behavior of the pentablock terpolymer in aqueous solution was examined by using turbidimetry, shear viscosity, rheo-small angle light scattering (rheo-SALS), dynamic light scattering (DLS), and small angle neutron scattering (SANS). The turbidity measurements demonstrated that the formation of intermicellar structures and compaction of the complexes are function of both polymer concentration and temperature. The viscosity and rheo-SALS experiments elucidated the intricate interplay between building-up and breaking-up of interchain complexes under the influence of shear flow. The DLS experiments show the coexistence of small entities and interchain complexes at low temperatures and the evolution of large intermicellar structures at higher temperatures. At the highest temperatures, compaction of the complexes occurred. The results from SANS revealed significant temperature-induced changes of the copolymer structure on a semi-local dimensional scale.

Keywords: Pentablock terpolymers; Phase behavior; Thermoresponsive polymers

1. Introduction

Amphiphilic block copolymers with different architectures and chemical composition that self-assemble into micelles and form gels in the semidilute concentration regime in response to external stimuli are an important class of materials with many applications, including drug delivery systems, gene therapy, and “smart” surface coatings.[1-5] Among the triggering mechanisms for responsive block copolymers, temperature and pH are considered as the most important stimuli for various biological applications, such as drug or gene delivery, smart bioactive surfaces, and molecular recognition agents.[6, 7] Especially, the cationic block stimuli-responsive copolymers can interact electrostatically with anionic

proteins at physiological condition, which may not only lead to a sustained release without initial burst, but also protect the proteins from denaturing effects. In addition, the positively charged block copolymers may also form electrostatic complexes with the negatively charged plasmid DNA and cell membranes under physiological condition. The DNA-loaded responsive copolymers formed in situ may lead to a sustained, local gene-delivery system [8].

It is worth noting that the main challenges for a broad application of stimuli-induced self-assembling copolymers depend on factors such as the copolymer composition, molecular architecture, and hydrophobicity of the copolymer, as well as molecular weight and solution concentration. These factors play an essential role for the specific properties of copolymers, such as micellar structure of the copolymer in solution, proper assembly features, and biocompatibility, etc. [9]. There are relatively few papers describing the fundamental relationships between the architecture and chemical design of multifunctional block copolymers, and in what way these features will influence how they self-assemble and what kind of mesoscopic structures are formed. Furthermore, the interplay between electrostatic and hydrophobic/hydrophilic interactions of block segments on the aggregation behavior of copolymers has not been established for complex copolymers.

During the past decade, great attention has been paid to the field of self-assembly of responsive diblock and triblock copolymers, which exhibit aggregation behavior in aqueous solution upon tuning external solution conditions, such as temperature and pH [10-14]. In the past years, some studies have been reported on the adsorption of multifunctional pentablock terpolymers onto surfaces [15,16] and the behaviors of the pentablock copolymers in bulk solution [17-21]. However, there is a lack of investigations on the temperature-induced self-association behavior of multifunctional copolymers in solution. The reason for this shortage is probably that these copolymers have intricate morphologies due to the complexity of the macromolecular structure.

In recent years, some studies have been reported on self-assembly behavior of responsive pentablock terpolymers with functional groups added at both ends of the chain [22, 23]. For instance, Agarwal et al.[1] and Determan et al. [17] prepared thermo-responsive gel-forming pentablock terpolymers as a self-assembling polymeric gene delivery vector, composed of commercially available Pluronic® F127 (PEO-*b*-PPO-*b*-PEO) triblock copolymers in the center, and cationic poly(amine methacrylate) diblocks at both ends of the chain by using the atom transfer radical polymerization (ATRP) method. These copolymers exhibit temperature dependent micellization because of the block architecture and the copolymer displays a lower critical solution temperature (LCST). Huynh et al.[24, 25] prepared pH/temperature-sensitive injectable hydrogels of poly(β-amino ester)-poly(ε-caprolactone)-poly(ethylene glycol)-poly(ε-caprolactone)-poly(β-amino ester) (PAE-PCL-PEG-PCL-PAE) pentablock terpolymers; the gels were used for controlled insulin delivery. The cationic nature of PAE is used to make ionic complexes with the anionic insulin.

Poly(*N*-isopropylacrylamide) (PNIPAAM) is one of the most studied temperature responsive polymers, and it exhibits a LCST in aqueous solution at around 32 °C [26]. The closeness of the LCST of PNIPAAM to the physiological temperature makes it an appealing polymer for drug and gene delivery applications. By increasing the solution temperature towards the transition temperature, the hydrogen bonds stabilizing the structure at lower temperatures are disrupted and hydrophobic interactions are generated through the isopropyl groups, and formation of aggregates occurs. In this way, we have a copolymer with tunable self-assembling features [27].

In recent years, studies have appeared on the use of PNIPAAM as an ingredient block in multi-block copolymers, consisting of hydrophilic, hydrophobic, and charged block sequences. Our group has for some time worked on pentablock terpolymers of the type ABCBA, where C is the PEG-spacer, B the NIPAAM block, and A is a charged block [28,

29]. The results from previous studies on pentablock copolymers indicate that the charged end-groups play a vital role for the structural and rheological properties of the polymers in aqueous media. In addition, the length of the PEG-spacer is important for the type of micelles that are formed and how the micelles are interconnected at higher polymer concentrations and temperatures [28]. Our understanding of the temperature-induced supramolecular features of multifunctional copolymers is quite limited and a more detailed understanding of the self-organized structures is necessary. The aim of the present study is to gain more insight into the self-assembling behavior of pentablock copolymers with charged end-groups.

To accomplish this, a cationic ABCBA pentablock terpolymer with a different type of charged end-group than employed previously [29] was synthesized by ATRP. The self-assembling features of the pentablock copolymer poly (3-acrylamidopropyl) trimethyl ammonium chloride-*block*-poly(*N*-isopropylacrylamide)-*block*-poly(ethylene glycol)-*block*-poly(*N*-isopropylacrylamide)-*block*-poly(3-acrylamidopropyl) trimethyl ammonium chloride, abbreviated as P(AMPTMA)$_{14}$-*b*-P(NIPAAM)$_{66}$-*b*-P(EG)$_{77}$-*b*-P(NIPAAM)$_{66}$-*b*-P(AMPTMA)$_{14}$, were characterized in aqueous media with the aid of turbidimetry, shear viscosity, dynamic light scattering DLS) and small-angle neutron scattering (SANS) as function of polymer concentration and temperature. The results from these experimental methods will elucidate the competition between hydrophobic interactions and electrostatic forces to get a better understanding of the self-assembling process and how this process is influenced by temperature-induced changes of structure, size, and size distribution.

2. Experimental methods

2.1. Materials

The monomer *N*-isopropylacrylamide (NIPAAM, Acros) was recrystallized from a toluene/n-hexane mixture twice and dried under vacuum prior to use. Poly(ethylene glycol)

(M_n value of 3400), 2-bromoisobutyl bromide and copper(II) chloride were all purchased from Sigma-Aldrich Co. 3-Acrylamidopropyl) trimethylammonium chloride) (AMPTMA, Aldrich) was purified from the inhibitor rest present in the sample by precipitating it into cold acetone, followed by washing with cold acetone, and finally drying under vacuum overnight. Triethylamine (TEA, Aldrich) was dried over anhydrous magnesium sulfate (Aldrich), filtered, distilled under N_2, and stored over 4 Å molecular sieves. Copper (I) chloride (Aldrich) was washed with glacial acetic acid (Aldrich), followed by washing with methanol, diethyl ether and finally dried under vacuum and kept under N_2 atmosphere. *N*,*N*,*N*',*N*'',*N*''',*N*''''-(hexamethyl triethylene tetramine) (Me_6TREN) was synthesized according to a procedure described by Ciampolini. [30] The bis-functional macro-initiator from PEG derivative (Br-PEG_{3400}-Br) was prepared *via* reaction of PEG_{3400} with 2-bromoisobutyl bromide in the presence of triethylamine as depicted in Fig. 1. The repeating units of ethylene glycol (EG) are estimated from the proton NMR spectra of the fully esterified product (as described in details elsewhere [28, 29, 31]) to be 77 units for PEG_{3400}, and it was denoted as $P(EG)_{77}$. All water used in this study was purified with a Millipore Mill-Q system with a resistivity of 18 M Ω.cm.

2.2. Synthesis of the pentablock terpolymer

A simple "one-pot" two step ATRP was carried out for preparation of the pentablock copolymer with some modifications (Fig. 1) [12, 28, 29, 32]. Briefly, the polymerization was performed in a water/DMF (50:50, v/v) mixture at 25 ^{o}C, and the initiator/catalyst system in the mixture contained PEG-bis-functional macroinitiator (PEG-Bis-MI), CuCl, $CuCl_2$, and Me_6TREN (with molar feed ratio of ([NIPAAM] = 2 M, [NIPAAM]/[AMPTMA]/[PEG-Bis-MI]/[CuCl]/[$CuCl_2$]/[Me_6TREN] = 140/60/1/2/1.2/3.2). The polymer was prepared and purified under similar conditions as described in detail previously [28, 29, 33].

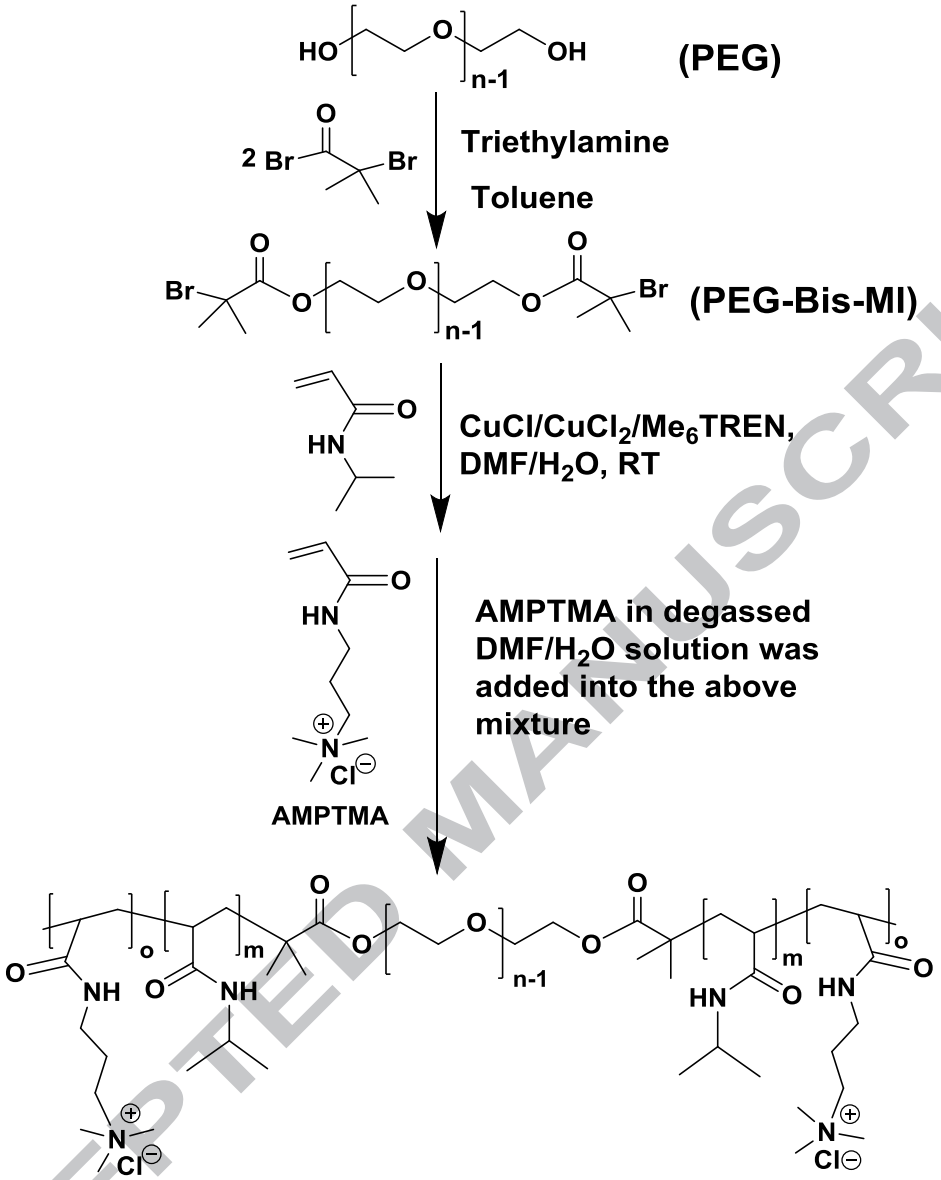

Fig. 1. Synthetic route for the preparation of the P(AMPTMA)$_{14}$-*b*-P(NIPAAM)$_{66}$-*b*-P(EG)$_{77}$-*b*-P(NIPAAM)$_{66}$-*b*-P(AMPTMA)$_{14}$ cationic pentablock terpolymer *via* the "one-pot" aqueous ATRP procedure.

The chemical structure and composition of the pentablock terpolymer was determined from its ^{1}H NMR spectrum as shown in Fig. 2. The number-average molecular weight and the unit numbers of *o*, *m*, and *n* in P(AMPTMA)$_o$-*b*-P(NIPAAM)$_m$-*b*-P(EG)$_n$-*b*-P(NIPAAM)$_m$-*b*-P(AMPTMA)$_o$ were determined by comparing the integral area of the methylene proton peak (**1**) of EG (δ = 3.70 ppm, -OCH_2CH_2O), the methylene proton peak (**5**) of PNIPAAM (δ =

3.85 ppm, C*H*$(CH_3)_2$), and the methylene proton (**12**) of AMPTMA (δ = 3.1 ppm, –N(C*H*$_3)_3$) obtained from its ^{1}H NMR spectrum. The entire repeating units of AMPTMA/NIPAAM/EG (2*o*/2*m*/*n*) are estimated to be *28/132/77*, based on our previous calculation results [12, 28, 29, 32, 34] that the number of repeating units of the ethylene glycol of PEG bis-MI is 77 for PEG_{3400}. Hence, the composition of the pentablock terpolymer is estimated to be *o/m/n/m/o* = *14/66/77/66/14*.

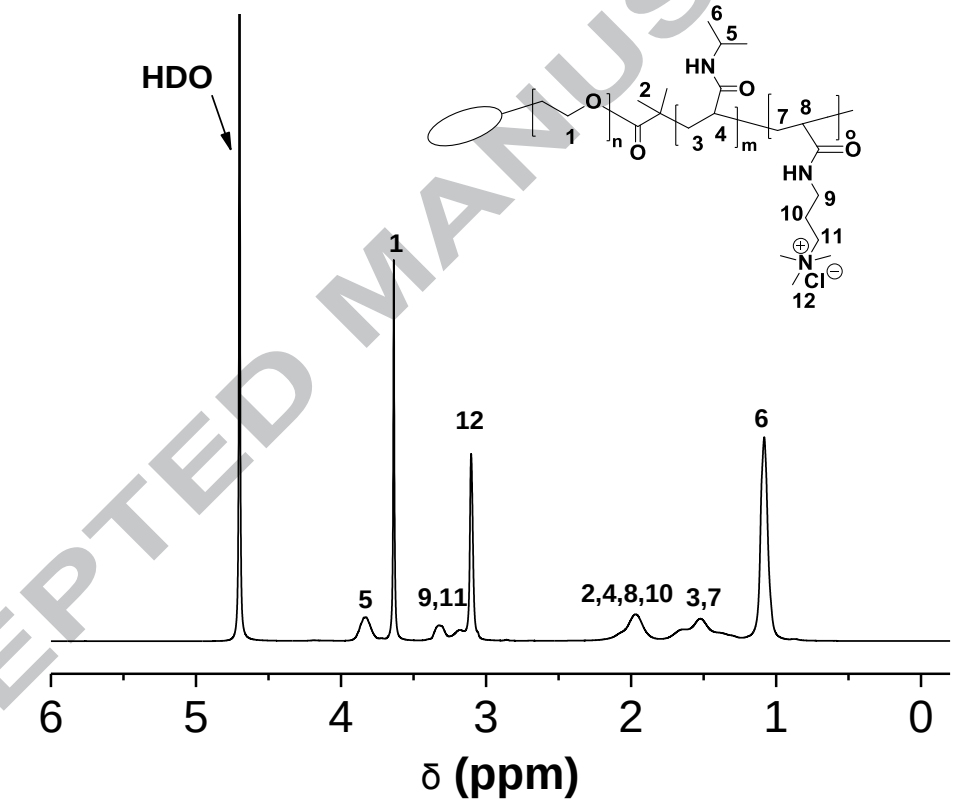

Fig. 2. ^{1}H NMR spectrum of the synthesized P(AMPTMA)$_{14}$-*b*-P(NIPAAM)$_{66}$-*b*-P(EG)$_{77}$-*b*-P(NIPAAM)$_{66}$-*b*-P(AMPTMA)$_{14}$ pentablock terpolymer (D_2O is used as the solvent, 300 MHz, 25 °C).

2.3. Asymmetric flow field-flow fractionation (AFFFF)

The number-average molecular weight (M_n), weight-average molecular weight (M_w), and polydispersity index (M_w/M_n) were determined by asymmetric flow field-flow fractionation (AFFFF). The AFFFF experiments [12] were conducted on an AF2000 FOCUS system

(Postnova Analytics, Landsberg, Germany) equipped with an RI detector (PN3140, Postnova) and a multi-angle (7 detectors in the range 35-145°) light scattering detector (PN3070, λ = 635 nm, Postnova). The terpolymer sample (0.5 wt % in 0.01 M NaCl) was measured using a 350 μm spacer, a regenerated cellulose membrane with a cut-off of 1000 (Z-MEM-AQU-425N, Postnova), and an injection volume of 20 μL. To minimize aggregate formation, the measurement was carried out at 10 °C. Processing of the measured data was achieved by the Postnova software (AF2000 Control, version 1.1.025). Weight-average molecular weight of the sample in the dilute concentration regime was obtained using this software with a Zimm-type fit, and a refractive index increment (dn/dc) of 0.156 cm^3/g (determined by using the RI-detector at 32 °C). The characteristic data of the studied pentablock terpolymer is displayed in Fig. 3. The result shows that the terpolymer has a fairly narrow molecular weight distribution.

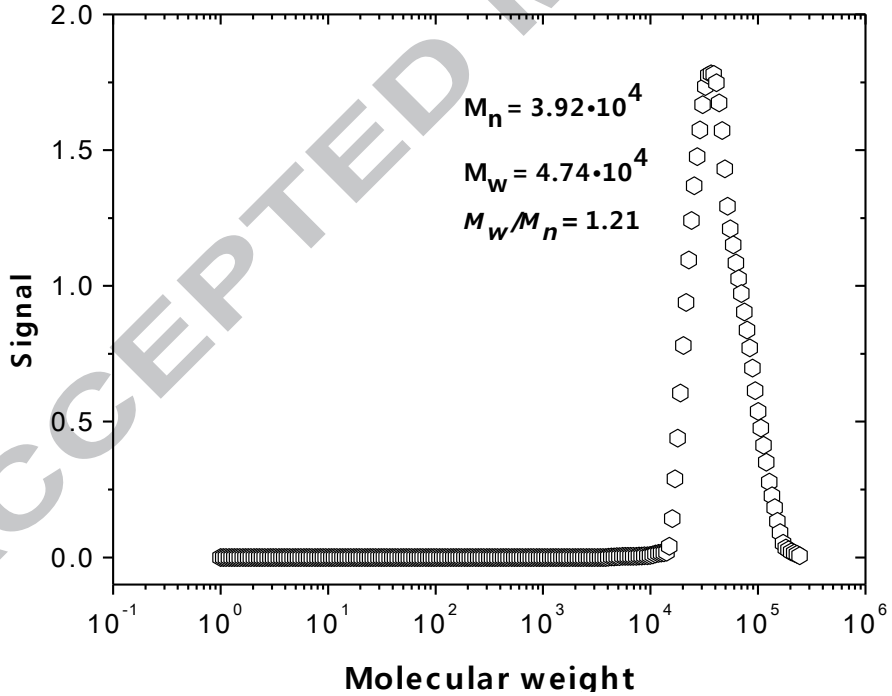

Fig. 3. The molecular weight distribution of the P(AMPTMA)$_{14}$-*b*-P(NIPAAM)$_{66}$-*b*-P(EG)$_{77}$-*b*-P(NIPAAM)$_{66}$-*b*-P(AMPTMA)$_{14}$ pentablock terpolymer in aqueous solutions (0.01 M NaCl) was determined by asymmetric flow field-flow fractionation (AFFFF).

2.4. Turbidimetry

Turbidimetry is a powerful method to disclose the association behavior in polymer solutions that exhibit a lower critical solution temperature. Temperature dependences of the turbidity of the terpolymer solutions at different concentrations were monitored at a heating rate of 1 °C min^{-1}, using an NK60-CPA cloud point analyzer from Phase Technology, Richmond, BC, Canada. A detailed description of this technique has been provided in an earlier publication [28]. The details of this equipment and the measurement procedure of turbidities have been described elsewhere[11]. Briefly, the function of the device is based on a scanning diffusive technique to characterize phase changes of the sample with high sensitivity. The light beam from an AlGaAs light source, operating at 654 nm, is focused on the measuring sample applied onto a glass plate coated with a thin metallic layer of very high reflectivity. Directly above the sample, an optical system with a light-scattering detector continuously monitors the scattered intensity signal (S) of the sample as it is subjected to prescribed temperature alterations. The relation between the signal from the cloud point analyzer and the turbidity (τ) is given by the following empirical equation, $\tau(cm^{-1}) = 9\times10^{-9}S^{3.751}$[31, 35]. The temperature at which the turbidity first start to deviate from the baseline was taken as the cloud point (CP) of the considered sample. The turbidity values were determined for solutions of different concentrations of the pentablock terpolymer in D_2O (0.1, 0.5, 4, and 8 wt%) in a temperature range from 25 to 60 °C. All measurements were performed at a heating rate of 1 K/min.

2.5. Shear viscosity and rheo-small angle light scattering (Rheo-SALS)

Simultaneous shear viscosity and small angle light scattering (Rheo-SALS) measurements were conducted using a Paar-Physica MCR 300 rheometer (Physica-Anton Paar), equipped with a specially designed parallel plate-plate configuration (plate diameter of

43 mm) in glass. In all experiments a 10 mW diode laser operating at a wavelength of 658 nm was employed as the light source, and a polarizer was placed in front of the laser and an analyzer below the sample, making both polarized (polarizer and analyzer parallel) and depolarized (polarizer and analyzer perpendicular) experiments possible.

The two-dimensional (2D) SALS images from the scattering patterns of the samples were captured using a CCD camera (driver LuCam V. 3.8), placed in a parallel position to the screen, and captured two-dimensional (2D) images. The time exposure for the acquisition of images was 200 ms; samples were placed between the two plates. The gap between the plates was 0.25 mm and this small distance reduces possible effects of multiple scattering. The temperature was gradually increased from 10 to 45 °C. A detailed description of this technique has been provided in an earlier publication [36]. The measuring apparatus is equipped with a temperature unit (Peltier plate), which provides an effective temperature control (±0.05 °C) for an extended time over the studied temperature range. The free surface of solutions was covered with a thin layer of low-viscosity silicone oil to prevent dehydration of the samples. It was tested that the viscosity value is practically not affected by the oil layer. All measurements were performed at a heating rate of 1 K/min.

2.6. Small angle neutron scattering (SANS)

The SANS measurements were conducted at selected temperatures in the range 30–50 °C on the SANS installation at the JEEP II reactor at IFE, Kjeller, Norway. The wavelength was set with the aid of a selector (Dornier), using a wavelength resolution $\Delta\lambda/\lambda = 10\%$. The neutron detector was a 128×128 pixel, He-3 filled RISØ-type detector, which is mounted on rails inside an evacuated detector chamber. The distance varied from 1.0 to 3.4 m and the wavelength between 5.1 and 10.2 Å, giving a wave-vector range from 0.008 to 0.3 $Å^{-1}$. Here q, the absolute value of the wave-vector, is given by $q=(4\pi/\lambda) \sin(\theta/2)$, where θ is the

scattering angle and λ is the neutron wavelength. The polymer solutions were held in 2 mm quartz cuvettes, equipped with stoppers. The measuring cells were placed onto a copper base for good thermal contact and mounted in the sample chamber.The transmission was measured separately, and absolute scattering cross section (cm^{-1}) was calculated by taking into account the contribution from empty cell and general background. The samples were prepared in heavy water instead of light water to enhance contrast and reduce incoherent background [28, 29].

2.7. Dynamic light scattering (DLS)

Dynamic light scattering (DLS) measurements were conducted with the aid of an ALV/CGS-8F multi-detector version compact goniometer system, with 8 fiber-optical detection units, from ALV-GmbH., Langen, Germany. Further experimental details of this equipment can be found in a previous work [36].

The DLS experiments were performed at different temperatures. The correlation function data were recorded continuously with an accumulation time of 2 min. The intensity correlation function was measured at 8 scattering angles simultaneously in the range 22-141^{o} with ALV/LSE-5004 multiple-τ digital correlator. Temperature in the measuring cell is controlled to within ±0.01 ^{o}C with a heating/cooling circulator. The copolymer solution was filtered in an atmosphere of filtered air through a 5 μm filter (Millipore) directly into precleaned NMR tubes. In the temperature range considered in this work, no problems with multiple scattering effects were encountered.

The experimentally recorded intensity autocorrelation function $g^2(q,t)$ is directly related to the theoretically amenable first-order electric field autocorrelation function $g^1(q,t)$ through the Siegert [37] relationship $g^2(q,t) = 1 + B|\, g^1(q,t)|^2$, where B (≤1) is an instrumental parameter and $q = (4\pi n/\lambda) \sin(\theta/2)$, where λ, θ, and n being the wavelength of the incident

light in a vacuum, scattering angle, and refractive index of the medium, respectively, is the wave-vector.

At temperatures up to approximately CP, the correlation functions can be described accurately by the sum of two stretched exponential functions as follows

$$g^1(t) = A_f \exp[-(t/\tau_{fe})^{\beta}] + A_s \exp[-(t/\tau_{se})^{\gamma}] \quad (1)$$

with $A_f + A_s = 1$. The parameters A_f and A_s are the amplitudes for the fast and the slow relaxation modes, respectively. The stretched exponents β and γ characterize the widths of the distribution of relaxation times for the fast and the slow mode, respectively. The variables τ_{fe} and τ_{se} are the relaxation times characterizing the fast and the slow relaxation process, respectively. At higher temperatures, when most of the unimers and micelles have been consumed in the formation of intermicellar structures, and the fraction of large species dominates, the correlation functions could be fitted with a single stretched exponential ($g^1(t) = \exp[-(t/\tau_{se})^{\beta}]$).

Bimodal relaxation processes have recently been reported [10,11,31,38] from DLS studies on associating polymer systems of various natures. In the analysis of the correlation functions with the aid of Eq. (1), a nonlinear fitting algorithm was employed to obtain best-fit values of the variables A_f, τ_{fe}, τ_{se}, β, and γ appearing on the right-hand side of Eq. (1). The fast relaxation time yields the mutual diffusion coefficient D_f ($\tau_f^{-1}=D_f q^2$) of unimers or micelles, whereas the slow relaxation time produces the mutual diffusion coefficient D_s of large clusters or intermicellar structures. Through the stretched exponents β ($0 < \beta \leq 1$) and γ ($0 < \gamma \leq 1$) the mean relaxation times for the fast and slow mode, respectively, are given by

$$\tau_f = \frac{\tau_{fe}}{\beta}\Gamma\left(\frac{1}{\beta}\right) \quad (1a)$$

$$\tau_s = \frac{\tau_{se}}{\gamma}\Gamma\left(\frac{1}{\gamma}\right) \quad (1b)$$

where Γ is the gamma function. From the relaxation modes, we are able to determine the apparent hydrodynamic radii ($R_{h,f}$ and $R_{h,s}$) from the fast and slow relaxation times, respectively, via the Stokes-Einstein relation $R_h = k_BT/6\pi\eta_0D$, where k_B is the Boltzmann constant, T is the temperature, η_0 is the solvent viscosity, and D is the mutual diffusion coefficient of unimers or micelles/intermicellar complexes. We should note that the Stokes-Einstein relation is strictly valid only in the absence of interparticle interactions and internal motions, that is, $qR_h < 1$. For some very large species considered in this study, this criterion is not fulfilled and some corrections to R_h should be made to obtain accurate values of R_h. However, since we are more concerned with the characteristic growth of clusters with increasing temperature, rather than the real cluster size itself, this correction is not crucial.

3. Results and discussion

3.1. Turbidity and phase separation

Results from the tubidity measurements on solutions of the pentablock copolymer at various concentrations are displayed in Fig. 4 (a-d). As expected, the temperature-induced transition of the turbidity is sharp when the cloud point is approached; the transition is significantly affected by the polymer concentration (0.1 wt% to 8 wt%). The rise of the turbidity at elevated temperatures signalizes the formation of intermicellar structures as a result of enhanced sticking probability and hydrophobic interactions induced mainly by the PNIPAAM microdomains in the clusters [42]. This shows that the charge density generated

by the PAMPTMA blocks is not enough to electrostatically stabilize the micelles at higher temperatures.

Fig. 4(a-d) show that as the polymer concentration increases, a progressively stronger temperature dependence of the turbidity evolves, and the transition takes place at lower temperatures. Figure 4e reveals that the cloud point drops as the polymer concentration rises. This type of behavior has been reported [27, 40, 41] in the past for solutions of amphiphilic copolymers containing PNIPAAM**.** As a result of increasing polymer concentration, the average distance between the moving entities is shorter; this leads to a higher collision frequency of the species through Brownian motion, augmenting the sticking probability. Hence, the formation of interchain aggregates occurs at a lower temperature. Although the cloud point of PNIPAAM falls off both with increasing molecular weight and polymer concentration [40], it seems that the cloud point at corresponding conditions is significantly higher for this multifunctional copolymer than for the PNIPAAM homopolymer. This can probably be ascribed to the charged endgroups and the PEG-spacer that make the copolymer more hydrophilic.

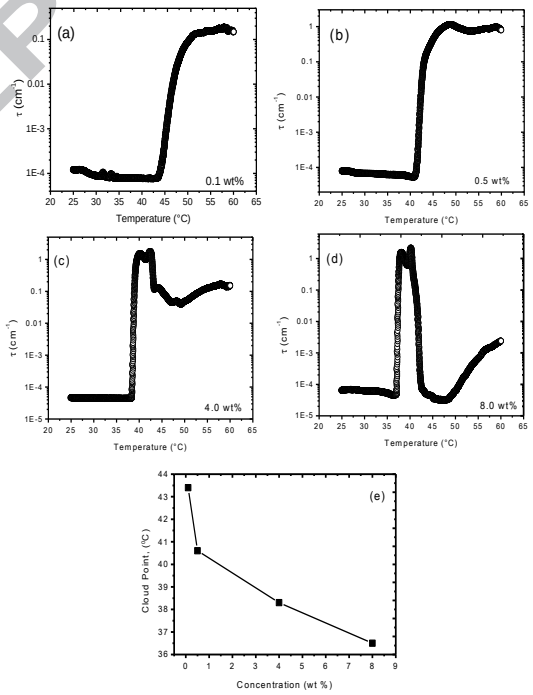

Fig. 4. (a-d) Temperature dependence of the turbidity for solutions of the pentablock copolymer at the concentrations indicated. (e) Effect of concentration on the cloud point.

The effects of concentration and temperature on the formation of aggregates in polymer solutions have been described in several theoretical studies [43-46]. In the framework of these approaches, the observed depression of the cloud point with rising polymer concentration can be interpreted in terms of the effective Flory-Huggins interaction parameter $\chi_{eff,}$ which is a function of both temperature and concentration. At a given temperature, the rise of χ_{eff} as the polymer concentration increases is attributed to poorer solvent conditions, or association of self-assembled moieties**.** Thus, the aqueous polymer solution at room temperature exhibits good solvent features at low polymer concentration and poor solvent conditions at high concentration. However, the general idea about thermoresponsive block copolymers containing PNIPAAM segments is that below the LCST, the isopropyl groups of PNIPAAM are surrounded by water, whereas above the LCST the hydrophobic groups are in contact with water and polymer segments, giving rise to augmented turbidity and growth of hydrophobic associations among PNIPAAM chains.

The turbidity results depicted for the higher two polymer concentrations (Fig. 4c and d) show that the turbidity curves pass through a maximum, and that the turbidity falls off strongly at higher temperatures; suggesting that the solutions become more transparent – an effect that can also be observed by visual inspection. This type of behavior has been reported in the past for solutions of amphiphilic copolymers [12, 27,39].

Our hypothesis is that the rise of the turbidity to the maximum is ascribed to the formation of large interchain complexes that penetrate each other to establish the connectivity in the network at sufficiently high concentration, or the long PEG-spacer allows bridging of micelles and this leads to a network of bridged and interpenetrating chains. The substantial drop of the turbidity at higher temperatures, especially for the highest concentration, might

then be due to the hydrophobic microdomains becoming more evenly distributed in the clusters [28]. An alternative explanation for the drastic change of the turbidity may be that above a certain minimum concentration, the total hydrophobicity becomes sufficiently large to induce a significant dehydration and concomitant compression of the species with increasing temperature. The corresponding reduction in size can result in a considerable drop in turbidity.

3.2. Shear viscosity and rheo small angle light scattering

The rheo-SALS technique is a powerful method that can provide useful information on a microscopic dimensional scale about shear-induced aggregation of sticky moieties and the formation of network. In Fig. 5, effects of temperature and shear rate on the viscosity of the pentablock copolymer solutions of different concentrations at a heating rate of 1 °C min^{-1} are illustrated.

At the lowest polymer concentration (0.1 wt%), the monotonous viscosity increase (Fig. 5a) at the different shear rates suggests that association structures are not disrupted by the shear rates in this domain, but the trends remind about the features observed from the quiescent turbidity experiments at the same concentration. The modest effect of shear rate on the shear viscosity at this concentration may indicate that the aggregates formed at elevated temperatures are compact and hard to break. At a concentration of 0.5 wt% (Fig. 5b), the viscosity curves pass through maxima and the amplitude of the peak decreases with increasing shear rate. To rationalize this finding, we need to recall that shear rate may both induce association aggregation and breakup of association complexes. The former effect is related to the Ortho-kinetic process, where shear rate speeds up the collision frequency over that originated from Brownian motion at quiescent conditions; this may generate a faster growth of the aggregates. At the same time, shear rates can break up aggregates. This is nicely

exemplified in Figure 5b, where associations are first built up and when they are sufficiently large, the shear rate disrupts the association complexes. Both the buildup and breakup of the association structures are dependent on the magnitude of the shear rate.

Similar profiles of the viscosity curves are observed for the higher two concentrations (Fig. 5c, d) and the growth and disruption of the aggregates are clearly visible. At the highest concentration (8 wt%), the silhouette of the viscosity curve and the location of the maximum are consistent with the features of the corresponding turbidity curve. In spite of that the considered shear rates are fairly low, the impact of shear rate on the cluster breakup is pronounced and this suggests that the association structures are rather fragile. The prominent upturn of the viscosity at the higher temperatures for the higher two polymer concentrations can be interpreted in the following way. When the association complexes have been disintegrated at intermediate temperatures, the sticking probability increases with increasing temperature and the shear forces are not strong enough to prevent further aggregation. The strong upturn of the viscosity at the highest temperatures is therefore an endorsement of an additional aggregation process. This is further addressed in connection with the analysis of the DLS results.

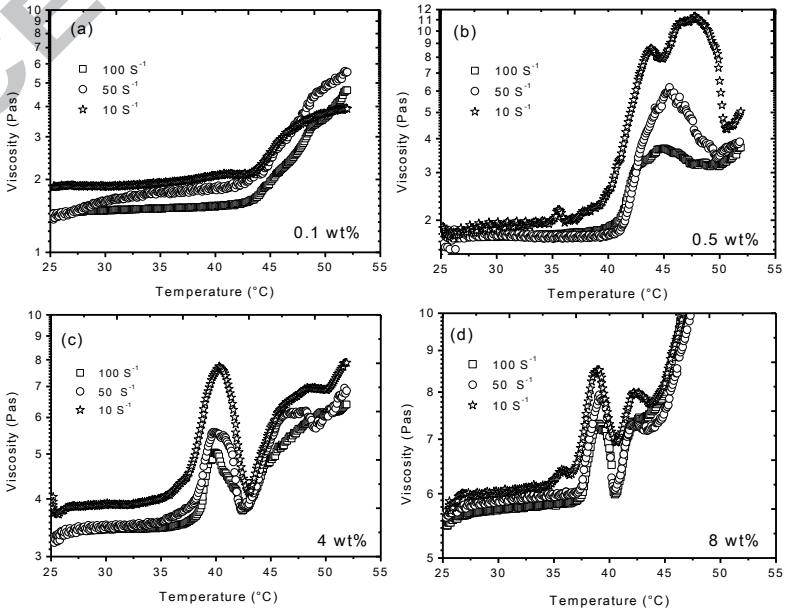

Fig. 5. Effects of temperature and polymer concentration on the shear viscosity of aqueous solutions of P(AMPTMA)$_{14}$-*b*-P(NIPAAM)$_{66}$-*b*-P(EG)$_{77}$-*b*-P(NIPAAM)$_{66}$-*b*-P(AMPTMA)$_{14}$ pentablock terpolymer solutions at various shear rates and concentrations.

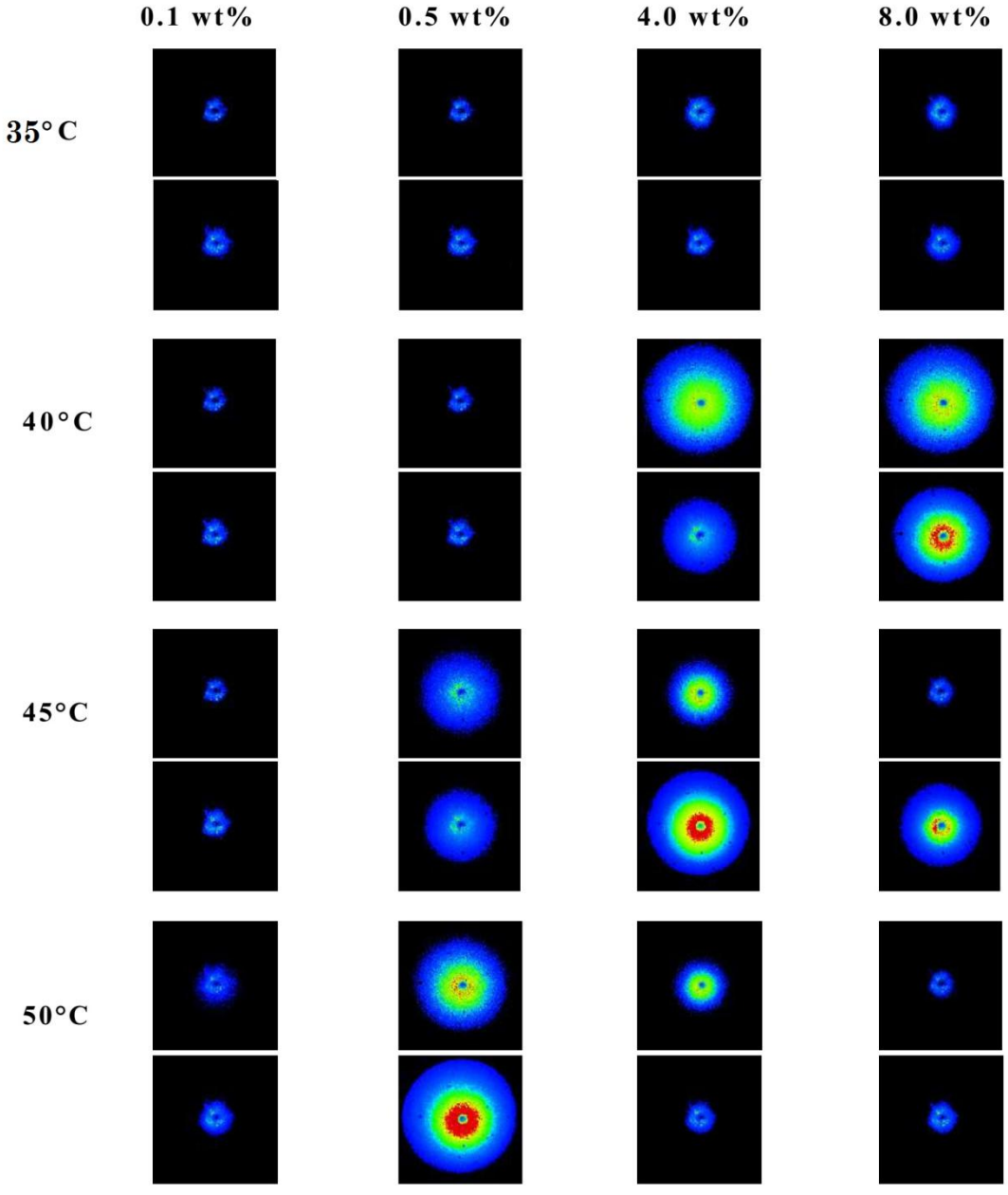

Fig. 6. 2D SALS scattering patterns of P(AMPTMA)$_{14}$-*b*-P(NIPAAM)$_{66}$-*b*-P(EG)$_{77}$-*b*-P(NIPAAM)$_{66}$-*b*-P(AMPTMA)$_{14}$ pentablock tercopolymer solutions of different concentrations at zero shear and shear rate of 50 s^{-1} (the upper and lower rows at each temperature are 0 s^{-1} and 50 s^{-1}, respectively) and at the indicated temperatures.

In Fig. 6, 2D SALS scattered intensity patterns have been recorded for various copolymer concentrations and temperatures, and at zero shear and shear rate of 50 s^{-1}). For the lowest polymer concentration (0.1 wt%), the images disclose that the effects of temperature and shear rate are moderate, as also suggested from the turbidity and viscosity results for this concentration. At 0.5 wt%, the change of the scattered intensity patterns is evident, especially at 45 ^{o}C and above; the impact of shear rate is pronounced at 50 ^{o}C, but modest at the other temperatures.

At 4 wt% and quiescent conditions, the scattered intensity images reveal that the intensity increases up to approximately 40 ^{o}C, whereas at 50 ^{o}C it seems to decrease and this is consistent with the trend observed for the turbidity (cf. Fig. 4c). The shear rate seems to promote cluster growth at 45 ^{o}C, whereas at 50 ^{o}C the shear rate seems to break up the association clusters. At 8 wt% polymer concentration, the general trend is that the scattered intensity rises up to 40 ^{o}C; after that the intensity falls off in agreement with the turbidity results for this concentration (Fig. 4d). A conspicuous effect of the shear rate is observed at 45 ^{o}C, where a moderate shear rate promotes the cluster growth, whereas at 50 ^{o}C no visible effect of the shear rate can be traced. Although the shear viscosity measurements on the 8 wt% sample (see Fig. 5d) show a boosted viscosity at 50 ^{o}C, the SALS result at the same condition suggests smaller association complexes and at a first glance this does not seem to be compatible with the results from the shear viscosity data. However, this apparent discrepancy can be rationalized in the following way. If we assume that there are growing interconnected complexes consisting of compressed hydrophobic microdomains at 50 ^{o}C, these complexes will of course contribute to the overall viscosity response, leading to an augmented viscosity. When it comes to SALS, the scattered intensity will be strongly dominated by the contribution

from the contracted hydrophobic microdomains and therefore the rest of the interconnected complex will not contribute much to the scattering profile. As observed from the DLS experiments below, a low fraction of large species is also present at low temperatures. A further discussion on this issue is given in connection with the analyses of the SANS and DLS results.

The general picture that emerges from rheo-SALS and viscosity experiments is that for small sticky species (elevated temperatures) shear rate may favor the growth of complexes, whereas for large interchain complexes many of them will be broken up under the influence of shear forces.

3.3. Dynamic light scattering

The light scattering data were recorded continuously at a heating rate of 0.2 ^{o}C/min and the temperature refers to the mean temperature during an experiment. Normalized correlation functions at a scattering angle of 73^{o} for 8 wt% solutions of the copolymer are displayed in Fig. 7a in the form of semilogarithmic plots. We have focused on this sample in DLS and SANS experiments below because the other used experimental methods suggest that most temperature-induced alterations occurred for this sample. Slow heating rates were utilized to avoid significant temperature-induced changes during accumulation of the correlation functions. To take into account trivial changes of the solvent viscosity (η_o) with temperature (T), the correlation function data have been plotted against tT/η_o. The general trend for the sample is that the tail of the correlation function is shifted toward longer times as the clusters grow at elevated temperatures. An inspection of the correlation functions reveals at low temperatures (25 and 30 ^{o}C) a bimodal appearance, which can well be described by two stretched exponentials (see Eq. (1)). This suggests that we have two populations of species of different size. At high temperatures the fast mode fades away and the decay of the correlation

function can be portrayed by a single stretched exponential. This finding suggests that the size and number of the formed aggregates increase and the impact of the small entities (unimers) is strongly reduced. As a result it is not possible to extract the fast relaxation mode.

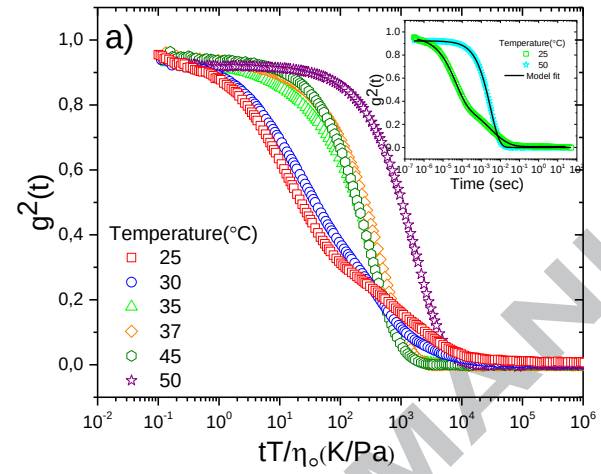

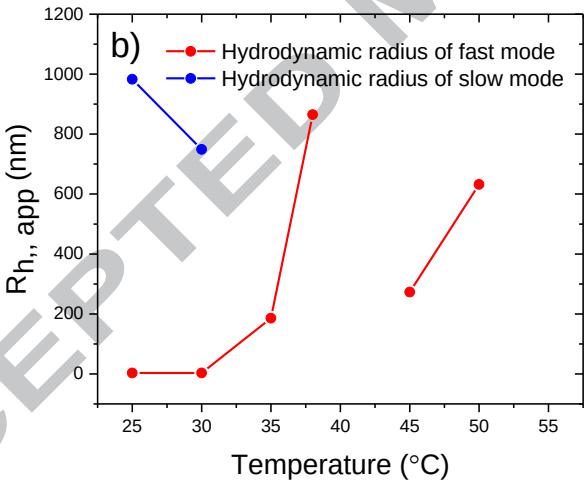

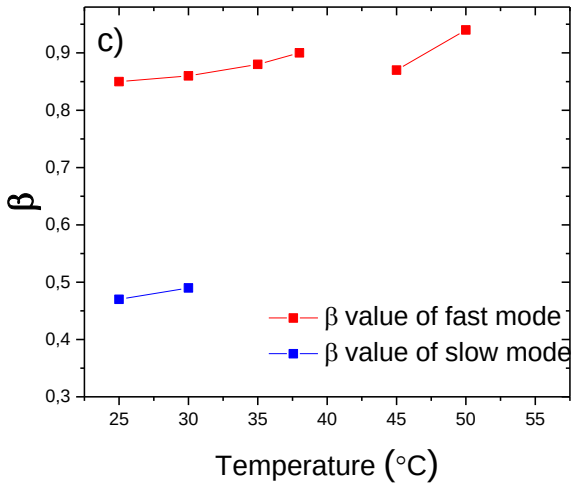

Fig. 7. a) Plot of the normalized intensity correlation function versus tT/η_o at a scattering angle of 73^o for the copolymer at a concentration of 8 wt% and the temperatures indicated. The inset shows fitted correlation data at a low and a high temperature. b) Temperature dependencies of the apparent hydrodynamic radii determined from the fitting by employing Eq. (1) for the fast relaxation time $R_{h,f}$ and the slow relaxation time $R_{h,s}$ through the Stokes-Einstein relationship for 8 wt% solution of the copolymer. The absence of data points in the intermediate temperature interval is due to multiple scattering problems. At high temperatures, the correlation functions were well-fitted by using a single stretched exponential. c) The temperature dependence of the stretched exponents obtained from the fitting for the copolymer at 8 wt%.

Figure 7b shows the temperature dependences of the apparent hydrodynamic radii, corresponding to the fast mode ($R_{h,f}$) and the slow mode ($R_{h,s}$) for the 10 wt% sample. The hydrodynamic radius representing the slow relaxation mode is only visible at the lower two temperatures. By using Eq. (1) in the fitting of the correlation function data for these two temperatures, it is found that the amplitude of the slow relaxation mode is low, suggesting a low population of large interchain complexes (Fig. 7b) at low temperatures. The low values of the stretched exponent (see Fig. 7c) for the slow mode at these conditions indicate that association complexes have a broad size distribution. These aggregates probably consist of micelles and multimolecular micelles [42]. The fast relaxation mode at these temperatures yields an apparent hydrodynamic radius of approximately 3 nm (unimer size) and the size distribution is rather narrow. At higher temperatures, the correlation function is monomodal and the decay can be described by a single stretched exponential (the inset of Fig. 7a). The apparent hydrodynamic radius increases monotonously as the temperature increases and large clusters are formed (Fig. 7b). The lack of data points in the interval 40-45 ^{o}C in Fig. 7b,c is due to problems with multiple scattering in DLS. In this temperature range the sample becomes very turbid and the amplitude of the intensity correlation function drops and the results are unreliable. At higher temperatures the solution is fairly transparent and the size of the species is smaller than prior to the transition region (fig. 7b). It is interesting to note that

the high values of the stretched exponent (ca. 0.9, Fig. 7c) at elevated temperatures suggest that the clusters have a fairly narrow size distribution.

We may conclude from these findings that at low temperatures unimers and a small fraction of large clusters coexist; at higher temperatures the large clusters totally dominate and the decay of the correlation function is well described by a single stretched exponential and a rather narrow size distribution of the species. At 45 ^{o}C, a compaction of the clusters occurs. Finally at 50 ^{o}C there is a subsequent increase of the effective cluster size and this trend is especially compatible with the shear viscosity results.

3.4. Small angle neutron scattering

To gain information about structure on a mesoscopic dimensional scale, SANS experiments were carried out on the 8 wt% sample at different temperatures, both below and above the transition temperature found from the turbidity measurements. Fig. 8 shows the reduced SANS intensity profiles at three different temperatures (30, 40, and 50 ^{o}C) for the 8 wt% sample in a semi-logarithmic representation. A noticeable feature is the vivid alteration of the SANS pattern with increasing temperature. The scattered intensity at low q increases more than a factor of ten upon each rise in temperature; this is strong indication of that structural reorganization takes place on the semi-local scale regime probed by SANS.

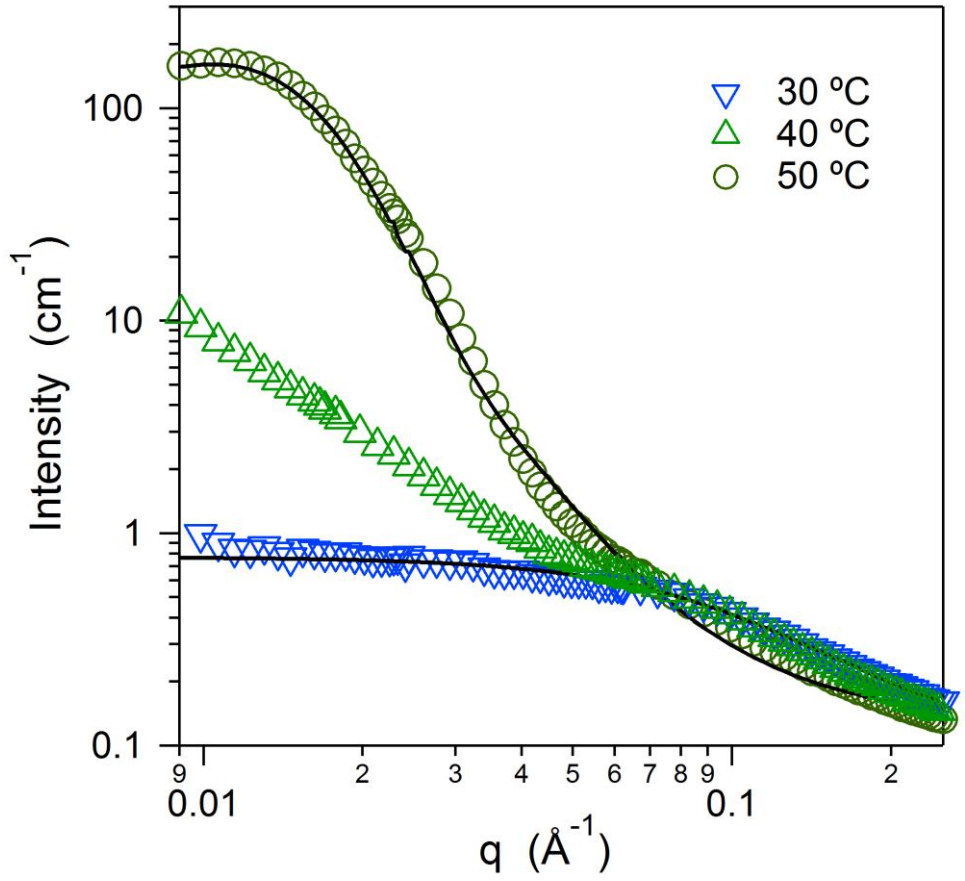

Fig. 8. SANS scattered intensity profile as a function of scattering vector for 8 wt% solution ofP(AMPTMA)$_{14}$-*b*-P(NIPAAM)$_{66}$-*b*-P(EG)$_{77}$-*b*-P(NIPAAM)$_{66}$-*b*-P(AMPTMA)$_{14}$ pentablock terpolymer at the indicated temperatures. The solid lines represent models fitted to the collected data (details of the fitted models are given in the text).

At 30 ^{o}C, that is below the threshold temperature observed from the turbidity results (Fig. 4d), only a weak small-angle scattering is found with respect to the surroundings as expected for unfolded individual chains. This situation can be portrayed by employing the Debye model, i.e., the form factor developed for a linear polymer chain in dilute solution, where the scattering function is given by $P(x) = 2[\exp(-x) + x-1]/x^2$, where $x= (qR_g)^2$ and R_g is the radius of gyration. From the data fitting, a value of R_g=16 Å is obtained. It is interesting to note that in spite of that the concentration is fairly high; the entities probed by SANS seem to be molecularly dispersed at this temperature. This parallels the small entities observed from DLS. Regardless of that the DLS results for this temperature disclose the existence of a small

population of huge clusters coexisting with a big fraction of very small entities, SANS is not capable of detecting this small portion of large aggregates. The reason for this is probably that the size of the items is outside the nanoscale window explored by SANS combined with the small number of such items present.

In the vicinity of the threshold temperature (40 ^{o}C), as emerged from the turbidity results (see Fig. 4d), the strong upturn of the scattered SANS intensity at low q-values is typical of that of large structures; there is no indication of a plateau at the lowest q-domain accessible in these experiments (Fig. 8). This suggests that the structures have sizes well above 1/q (min), *i.e.*, approx. 1/0.008 Å^{-1}, or 125 Å. The actual sixe cannot be estimated from the SANS profile since there is no characteristic flattening at the lowest available q-values. Although the turbidity method operates on a macroscopic dimensional scale and the influence of sizes cannot be compared with those deduced from SANS, the drastic turbidity rise in this region, as depicted in Figure 4d, portends the existence of large structures and this is reflected in the SANS results (see also the discussion of the DLS results above).

At a temperature above the transition region (50 ^{o}C), a conspicuous change in the profile of the scattering curve is observed in comparison to the profiles at the lower temperatures. The scattered intensity is strong and a plateau region is developed at low q-values. The fact that much of the scattered intensity has now moved into the region above q=0.01 Å^{-1}, suggests that the probed structures have characteristic sizes that are considerably smaller than those detected in the transition domain, where a strong upturn was found in the scattered intensity curve.

The shape of the scattered intensity profile and the inherent properties of this copolymer encouraged us to test a core-shell model to fit the high-temperature SANS data. The conjecture is that the species are made up of a central region (“core”) of hydrophobic segments, and the shell consists of hydrophilic PEG chains protruding out from this domain.

Because of the charges of the polymer, it is necessary to implement a Coulomb interaction potential in this model. By using the core-shell form factor, together with a screened Coulomb interaction potential, a reasonable fit is obtained (cf. Fig. 8) yielding a core radius of 103 Å and a shell thickness 7 Å. This corresponds to an overall cluster diameter of 220 Å. In this calculation we have used the already known values of temperature, D_2O scattering length density, and dielectric constant, i.e., at 328 K, $6.3 \cdot 10^{-6}$ Å^{-2} and 78, respectively. The strong increase in the scattered SANS intensity at 50 ^{o}C compared to that at 30 ^{o}C, can be rationalized in the following way. At 30 ^{o}C, the moieties exist as unimers (R_g=16 Å), whereas at 50 ^{o}C (R=110 Å) intermicellar structures are formed. The huge alteration in the scattered intensity can probably be ascribed to both the larger size of the clusters and the high density of the segments inside the core as an effect of the temperature-induced compaction of the clusters. The contraction of the moieties at the highest temperature probably generates a sufficient size reduction of the species to move them into the q-window accessible for SANS. At 40 ^{o}C, the hydrophobic microdomains are most likely too large so they fall outside the nanoscale domain covered by SANS.

A few years ago [28], our group studied a very similar pentablock terpolymer ($P(SSS)_{14}$-*b*-$P(NIPAAM)_{65}$-*b*-$P(EG)_{77}$-*b*-$P(NIPAAM)_{65}$-*b*-$P(SSS)_{14}$). The major difference is that the present copolymer ($P(AMPTMA)_{14}$-*b*-$P(NIPAAM)_{66}$-*b*-$P(EG)_{77}$-*b*-$P(NIPAAM)_{66}$-*b*-$P(AMPTMA)_{14}$) contains positively charged end-groups instead of negatively charged ones and the nature of the end-groups is different. However, in spite of the different charged end-groups the present SANS experiments reveal that this copolymer behaves similarly to the pentablock copolymer studied earlier. The features and the temperature-induced changes observed for the present copolymer suggest that the structural findings detected on a semi-local dimensional scale follow the same principles as found previously. This indicates that the

type of charged group is not important for the mesoscopic structural behavior of this multi-block copolymer.

4. Conclusions

In this work, self-assembling of a positively charged thermoresponsive amphiphilic pentablock terpolymer, P(AMPTMA)$_{14}$-*b*-P(NIPAAM)$_{66}$-*b*-P(EG)$_{77}$-*b*-P(NIPAAM)$_{66}$-*b*-P(AMPTMA)$_{14}$, has been investigated at quiescent conditions and under the influence of shear rates at various temperatures by utilizing turbidimetry, shear viscosity, rheo-SALS, DLS, and SANS experiments. At quiescent conditions, the turbidity results show temperature-induced formation of association complexes and the intensity of this process rises with increasing polymer concentration; the cloud point drops as the concentration increases. A special interesting feature was detected at the highest concentration (8 wt%), where a distinct transition peak evolved in the turbidity data; suggesting that large clusters (micelles and intermicellar clusters) are developed at intermediate temperatures, and a substantial contraction of the flocs. At low temperatures, the DLS results show that unimers coexist with a small fraction of large clusters. At higher temperatures (up to ca. 40 ^{o}C), a strong growth of the clusters is observed; still higher temperatures lead to compaction of the clusters and they have a quite narrow size distribution.

The SANS experiments conducted on the 8 wt% sample suggested that we have molecularly dispersed entities with a radius of gyration of ca. of 16 Å at temperatures prior to the transition zone. At temperatures in the transition region, SANS revealed a strong upturn of the scattered intensity at low q-values; suggesting the creation of large aggregates with sizes that are too big to be determined by SANS. At higher temperatures, outside the transition region, a different situation emerges where the scattered intensity profile can be portrayed by a core-shell model. The radius of the core is about 103 Å and the thickness of the corona is ca. 7 Å. The DLS measurements provide us with global structures of sizes that are too large to be

probed by SANS; thus the sizes determined from SANS are from sub-structures in the nanoscale window accessible by SANS.

The rheo-SALS data divulge isotropic scattered intensity patterns at all studied conditions of temperature and polymer concentration. The scattered intensity features at different shear rates demonstrate that at low temperatures shear-induced growth of association complexes is promoted, whereas at elevated temperatures shear stresses generate destruction of flocs. The shear viscosity measurements clearly revealed the omnipresent competition between buildup of association complexes and breakup of these complexes. Depending on polymer concentration, temperature, and shear rate, one of these factors will dominate. At temperatures around 50 ^{o}C for the 8 wt% sample, large association structures are built up and they are not affected by the shear rates considered in this study.

The results from this work have exposed the intricate interplay between hydrophilic, hydrophobic and electrostatic interactions. It is obvious that a thorough understanding of this interplay is necessary to be able to use these systems for medical applications, such as gene delivery and carriers for drugs.

AUTHOR INFORMATION

Corresponding author

E-mail bo.nystrom@kjemi.uio.no, Phone: +47-22855522

Notes

The authors declare no competing financial interest.

Acknowledgements

BN acknowledges financial support from Norwegian Financial Mechanism 2009-2014 under Project Contract MSMT-28477/2014 (project 7F14009). B.N greatly appreciate the financial support of the European Union through the NanoS3 project (GrantNo. 290251) of the FP7-PEOPLE-2011-ITN call.

References

[1] A. Agarwal, R. Unfer, S.K. Mallapragada, Novel cationic pentablock copolymers as non-viral vectors for gene therapy, J. Control. Release 103 (2005) 245-258.

[2] M. Lazzari, G. Liu, S. Lecommandoux, Block copolymers in nanoscience, John Wiley & Sons 2007.

[3] T. Schnitzler, A. Herrmann, DNA block copolymers: functional materials for nanoscience and biomedicine, Acc. Chem. Res. 45 (2012) 1419-1430.

[4] H. Hu, M. Gopinadhan, C.O. Osuji, Directed self-assembly of block copolymers: a tutorial review of strategies for enabling nanotechnology with soft matter, Soft Matter 10 (2014) 3867-3889.

[5] B. Claro, K. Zhu, S. Bagherifam, S.G. Silva, G. Griffiths, K.D. Knudsen, E.F. Marques, B. Nyström, Phase behavior, microstructure and cytotoxicity in mixtures of a charged triblock copolymer and an ionic surfactant, Eur. Polym. J. 75 (2016) 461-473.

[6] P. De, M. Li, S.R. Gondi, B.S. Sumerlin, Temperature-regulated activity of responsive polymer−protein conjugates prepared by grafting-from via RAFT polymerization, J. Am. Chem. Soc. 130 (2008) 11288-11289.

[7] J. Chen, M. Liu, C. Gao, S. Lü, X. Zhang, Z. Liu, Self-assembly behavior of pH-and thermo-responsive hydrophilic ABCBA-type pentablock copolymers synthesized by consecutive RAFT polymerization, RSC Adv. 3 (2013) 15085-15093.

[8] N. Li, L. Zhao, L. Qi, Z. Li, Y. Luan, Polymer assembly: Promising carriers as co-delivery systems for cancer therapy, Prog. Polym. Sci. 58 (2016) 1-26.

[9] X. Han, X. Zhang, H. Zhu, Q. Yin, H. Liu, Y. Hu, Effect of composition of PDMAEMA-b-PAA block copolymers on their pH-and temperature-responsive behaviors, Langmuir 29 (2013) 1024-1034.

[10] A.-L. Kjøniksen, B. Nyström, H. Tenhu, Characterisation of thermally controlled chain association in aqueous solutions of poly (N-isopropyl acrylamide)-g-poly (ethylene oxide): Dynamic light scattering, Colloids Surf A Physicochem Eng Asp. 228 (2003) 75-83.

[11] A.-L. Kjøniksen, A. Laukkanen, C. Galant, K.D. Knudsen, H. Tenhu, B. Nyström, Association in aqueous solutions of a thermoresponsive PVCL-g-C11EO42 copolymer, Macromolecules 38 (2005) 948-960.

[12] K. Zhu, H. Jin, A.-L. Kjøniksen, B. Nyström, Anomalous transition in aqueous solutions of a thermoresponsive amphiphilic diblock copolymer, J. Phys. Chem. B 111 (2007) 10862-10870.

[13] S. Hocine, M.-H. Li, Thermoresponsive self-assembled polymer colloids in water, Soft Matter 9 (2013) 5839-5861.

[14] M.T. Calejo, A.M.S. Cardoso, A.-L. Kjøniksen, K. Zhu, C.M. Morais, S.A. Sande, A.L. Cardoso, M.C.P. de Lima, A. Jurado, B. Nyström, Temperature-responsive cationic block copolymers as nanocarriers for gene delivery, Int. J. Pharm. 448 (2013) 105-114.

[15] S. Peleshanko, K. D. Anderson, M. Goodman, M. D. Determan, S. K. Mallapragada, V.V. Tsukruk, Thermoresponsive reversible behavior of multistimuli Pluronic-based pentablock copolymer at the air-water interface, Langmuir 23 (2007) 25-30.

[16] T. Chen, Y. Lu, T. Chen, X. Zhang, B. Du, Adsorption of PNIPAmx-PEO20-PPO70-PEO20-PNIPAmx pentablock terpolymer on gold surfaces: effects of concentration, temperature, block length, and surface properties, Phys. Chem. Chem. Phys. 16 *(*2014) 5536--5544.

[17] M.D. Determan, J.P. Cox, S. Seifert, P. Thiyagarajan, S.K. Mallapragada, Synthesis and characterization of temperature and pH-responsive pentablock copolymers, Polymer 46 (2005) 6933-6946.

[18] M. D. Determan, L. Guo, P. Thiyagarajan, S. K. Mallapragada, Supramolecular self-assembly of multiblock copolymers in aqueous solution, Langmuir 22 (2006) 1469-1473.

[19] N. A. Hadjiantoniou, A. I. Triftaridou, D. Kafouris, M. Gradzielski, C. S. Patrickios, Synthesis

and characterization of amphiphilic multiblock copolymers: effect of the number of blocks on micellization, Macromolecules 42 (2009) 5492–5498.
[20] A. Mei, X. Guo, Y. Ding, X. Zhang, J. Xu, Z. Fan, B. Du, PNIPAm-PEO-PPO-PEO-PNIPAm pentablock terpolymer: synthesis and chain behavior in aqueous solution, Macromolecules 43 (2010) 7312–7320.
[21] Y. Lu, T. Chen, A. Mei, T. Chen, Y. Ding, X. Zhang, J. Xu, Z. Fana, B. Du, Phys. Chem. Chem. Phys. 15 (2013) 8276--8286.
[22] Y. He, T.P. Lodge, Thermoreversible ion gels with tunable melting temperatures from triblock and pentablock copolymers, Macromolecules 41 (2008) 167-174.
[23] G.J. Im, S.Y. Chae, K.C. Lee, D.S. Lee, Controlled release of insulin from pH/temperature-sensitive injectable pentablock copolymer hydrogel, J. Control. Release. 137 (2009) 20-24.
[24] D.P. Huynh, M.K. Nguyen, B.S. Pi, M.S. Kim, S.Y. Chae, K.C. Lee, B.S. Kim, S.W. Kim, D.S. Lee, Functionalized injectable hydrogels for controlled insulin delivery, Biomaterials 29 (2008) 2527-2534.
[25] M.K. Nguyen, B.S. Kim, D.S. Lee, Molecular design of novel pH/temperature-sensitive hydrogels, Polymer 50 (2009) 2565-2571.
[26] H. K. Schild, Poly(*N*-isopropylacrylamide): experiment, theory and application, Prog. Polym. Sci. 17 (1992) 163-249.
[27] S. Bayati, K. Zhu, L.T. Trinh, A.-L. Kjøniksen, B. Nyström, Effects of temperature and salt addition on the association behavior of charged amphiphilic diblock copolymers in aqueous solution, J. Phys. Chem. B. 116 (2012) 11386-11395.
[28] N. Beheshti, K. Zhu, A.-L. Kjøniksen, K.D. Knudsen, B. Nyström, Characterization of temperature-induced association in aqueous solutions of charged ABCBA-type pentablock tercopolymers, Soft Matter 7 (2011) 1168-1175.
[29] G. Isapour, R. Lund, K. Zhu, Z. Quan, K.D. Knudsen, B. Nyström, Schizophrenic micellization in aqueous solutions of the pH-and temperature responsive pentablock terpolymer PDEAEMAx-b-PNIPAAMy-b-PEGz-b-PNIPAAMy-b-PDEAEMAx, Eur. Polym. J. 70 (2015) 79-93.
[30] M. Ciampolini, N. Nardi, Five-coordinated high-spin complexes of bivalent cobalt, nickel, and copper with tris (2-dimethylaminoethyl) amine, Inorganic Chemistry 5 (1966) 41-44.
[31] A. Maleki, A.-L. Kjøniksen, K. Zhu, B. Nyström, Temperature-induced aggregation kinetics in aqueous solutions of a temperature-sensitive amphiphilic block copolymer, J. Phys. Chem. B. 115 (2011) 8975-8980.
[32] F. Kahnamouei, K. Zhu, R. Lund, K.D. Knudsen, B. Nyström, Self-assembly of a hydrophobically end-capped charged amphiphilic triblock copolymer: effects of temperature and salinity, RSC Adv. 5 (2015) 46916-46927.
[33] A.-L. Kjøniksen, K. Zhu, G. Karlsson, B. Nyström, Novel transition behavior in aqueous solutions of a charged thermoresponsive triblock copolymer, Colloids Surf A Physicochem Eng Asp. 333 (2009) 32-45.
[34] W. Wang, H. Mauroy, K. Zhu, K.D. Knudsen, A.-L. Kjøniksen, B. Nyström, S.A. Sande, Complex coacervate micelles formed by a C18-capped cationic triblock thermoresponsive copolymer interacting with SDS, Soft Matter 8 (2012) 11514-11525.
[35] H. Jonassen, A.-L. Kjøniksen, M. Hiorth, Effects of ionic strength on the size and compactness of chitosan nanoparticles, Colloid. Polym. Sci. 290 (2012) 919-929.
[36] A.-L. Kjøniksen, K. Zhu, R. Pamies, B. Nyström, Temperature-induced formation and contraction of micelle-like aggregates in aqueous solutions of thermoresponsive short-chain copolymers, J. Phys. Chem. B. 112 (2008) 3294-3299.
[37] A. J. F Siegert, Massachusetts Institute of Technology, Radiation Laboratory Report No. 465, 1943.
[38] H. Chen, X. Ye, G. Zhang, Q. Zhang, Dynamics of thermoresponsive PNIPAM-g-PEO copolymer chains in semi-dilute solution, Polymer 47 (2006) 8367-8373.
[39] J. Nambam, J. Philip, Thermogelling properties of triblock copolymers in the presence of hydrophilic Fe_3O_4 nanoparticles and surfactants, Langmuir 28 (2012) 12044-12053
[40] R. Pamies, K. Zhu, A.-L. Kjøniksen, B. Nyström, Thermal response of low molecular weight poly-(N-isopropylacrylamide) polymers in aqueous solution, Polym. Bull. 62 (2009) 487-502.

[41] R. Pamies, K. Zhu, S. Volden, A.-L. Kjøniksen, G. Karlsson, W.R. Glomm, B. Nyström, Temperature-induced flocculation of gold particles with an adsorbed thermoresponsive cationic copolymer, J. Phys. Chem. C. 114 (2010) 21960-21968.
[42] Y. Zhou, K. Jiang, Q. Song, S. Liu, Thermo-induced formation of unimolecular and multimolecular micelles from novel double hydrophilic multiblock copolymers of N,N-dimethylacrylamide and N-isopropylacrylamide, Langmuir 23 (2007) 13076-13084.
[43] A. Matsuyama, F. Tanaka, Theory of solvation-induced reentrant phase separation in polymer solutions, Physical review letters 65 (1990) 341.
[44] P.C. Painter, L.P. Berg, B. Veytsman, M.M. Coleman, Intramolecular screening in nondilute polymer solutions, Macromolecules 30 (1997) 7529-7535.
[45] V. Baulin, A. Halperin, Concentration dependence of the flory ξ parameter within two-state models, Macromolecules 35 (2002) 6432-6438.
[46] E. Dashtimoghadam, G. Bahlakeh, H. Salimi-Kenari, M.M. Hasani-Sadrabadi, H. Mirzadeh, B. Nyström, Rheological study and molecular dynamics simulation of biopolymer blend thermogels of tunable strength, Biomacromolecules 17 (2016) 3474-3484.

Graphical Abstract:

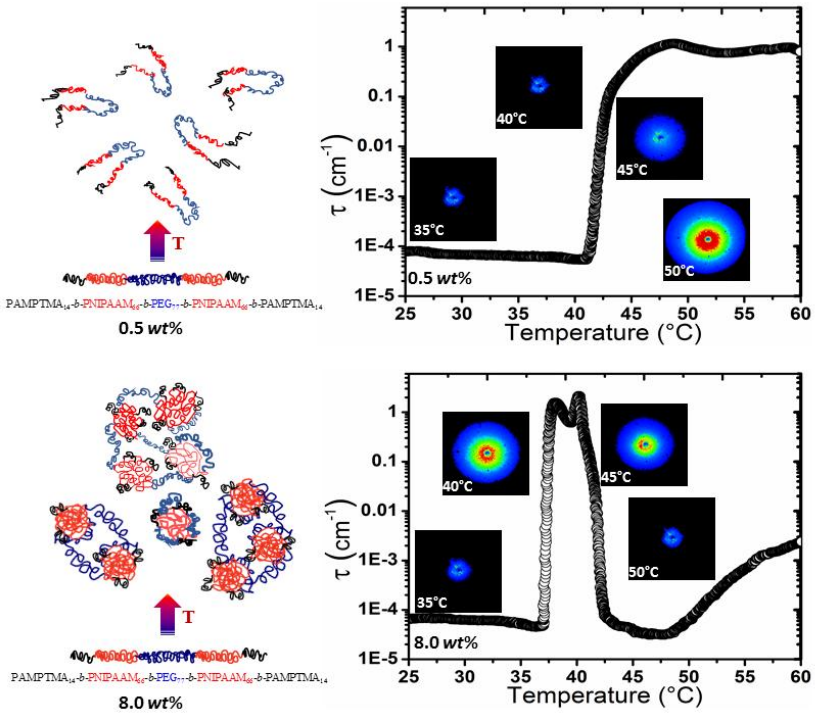

Highlights

- Self-assembling of a cationic temperature sensitive pentablock copolymer.
- Temperature-induced formation of micellar and intermicellar structures.
- Building-up and breaking-up of interchain complexes under the influence of shear flow.